Electronic Supplementary Information

A Pd-based plasmonic photocatalyst for nitrogen fixation through an antenna–reactor mechanism

Yuanyuan Yang,[a‡] Henglei Jia,*[a‡] Sihua Su,[c] Yidi Zhang,[a] Mengxuan Zhao,[a] Jingzhao Li,[a] Qifeng Ruan*[c] and Chun-yang Zhang*[ab]

[a] College of Chemistry, Chemical Engineering and Materials Science, Shandong Normal University, Jinan 250014, China.

[b] School of Chemistry and Chemical Engineering, Southeast University, Nanjing 211189, China.

[c] Ministry of Industry and Information Technology Key Lab of Micro-Nano Optoelectronic Information System & Guangdong Provincial Key Laboratory of Semiconductor Optoelectronic Materials and Intelligent Photonic Systems, Harbin Institute of Technology, Shenzhen 518055, China.

*Corresponding author. E-mail: hljia@sdnu.edu.cn (H. L. Jia), ruanqifeng@hit.edu.cn (Q. F. Ruan), cyzhang@sdnu.edu.cn and zhangcy@seu.edu.cn (C.-y. Zhang)

‡ These authors contributed equally to this work.

Supporting Experimental Section

Chemicals. Polyvinylpyrrolidone (PVP, MW = 55,000), L-Ascorbic acid (AA, ≥ 99%), sodium tetrachloropalladate(II) (Na_2PdCl_4, 98%), formaldehyde (HCHO, 37 wt%), Ruthenium(III) acetylacetonate ($Ru(acac)_3$, 97%) and methanol (CH_3OH, 99.9%) were purchased from Sigma-Aldrich. Potassium bromide (KBr, ≥ 99%), ethanol (C_2H_6O, 95%), hydrochloric acid (HCl, 36.0−38.0 wt%), iron(III) chloride ($FeCl_3$, 97%), hydrazine hydrate aqueous solution ($N_2H_4{\cdot}H_2O$, ≥ 50.0%) and sodium hydroxide (NaOH, ≥ 96.0%) were obtained from Sinopharm Chemical Reagent. Salicylic acid ($C_6H_4(OH)COOH$, 99%) and sodium hypochlorite solution (NaClO, available chlorine ≥ 5.0%) were obtained from Aladdin Reagent. Benzyl alcohol (C_7H_8O, ≥ 99%), glycerol ($C_3H_8O_3$, 99%) and sodium nitroferricyanide (III) dihydrate ($Na_2[Fe(CN)_5NO]{\cdot}2H_2O$, 99%) were purchased from Macklin. Dimethyl sulfoxide-d6 (DMSO-d6, (D, 99.9%) + 0.03% V/V TMS) was obtained from Cambridge Isotope Laboratories, Inc. Nitrogen ($^{14}N_2$, 99.999%), nitrogen ($^{15}N_2$, 98 atom% ^{15}N) and argon (Ar, 99.999%) were used as received. Deionized (DI) water with a resistivity of 18.2 MΩ·cm was used in all experiments.

Growth of the Pd nanocubes. The Pd nanocubes were prepared following a previous work.[1] Briefly, PVP (105 mg), AA (60 mg), and KBr (600 mg) were added into DI water (8.0 mL) in a vial and pre-heated to 80 °C in an oil bath under magnetic stirring for 10 min. Subsequently, Na_2PdCl_4 (0.58 M, 3 mL) was added into the mixture solution using a pipette and the vial was capped. The resultant solution was heated at 80 °C for 3 h. The product was collected by centrifugation, washed with water, and re-dispersed in DI water (10 mL) for future use.

Growth of the Pd nanooctahedrons. The Pd nanooctahedrons were prepared using a seed-mediated approach with Pd nanocubes as the seeds, as reported in previous work with modifications.[2] In a standard procedure, Na_2PdCl_4 solution (32.86 mM, 3.62 mL) was introduced into a mixture solution (8 mL) containing PVP (105 mg), HCHO (100 μL), and Pd nanocubes (18 nm in edge length, 0.3 mL), which had been heated at 60 °C for 10 min under magnetic stirring in a capped vial. The resultant solution was heated at 60 °C for another 3 h. After collection by centrifugation and washing with water, the final product was redispersed in benzyl alcohol (8 mL) for further use.

Preparation of the Pd octahedron/Ru array nanostructures. In a standard procedure, PVP (20 mg) was added into benzyl alcohol (8.0 mL) in a 25 mL three-neck flask and preheated to 180 °C in an oil bath for 10 min. Subsequently, Pd nanooctahedron sample (1 mL, in benzyl alcohol) was added in the three-neck flask using a pipette. After stirring for 5 min, $Ru(acac)_3$ solution (1.25 mg mL^{-1}, 2 mL, in benzyl alcohol) was injected into the flask at a

rate of 8 mL h^{-1} using a syringe pump. The reaction was allowed to proceed for an additional 15 min after the $Ru(acac)_3$ solution had been completed injected. The products were collected by centrifugation, washed with ethanol and finally redispersed in DI water (10 mL) for future use.

Preparation of the Pd cube/Ru nanostructures. The synthesis of the Pd cube/Ru nanostructures was similar to that of the Pd octahedron/Ru array nanostructures except that Pd nanooctahedrons were replaced by Pd nanocubes.

Preparation of hollow Ru nanoshells. The hollow Ru nanoshells were prepared by etching Pd core from the Pd octahedron/Ru array nanostructures. The etching solution was prepared by adding KBr (300 mg), $FeCl_3$ (50 mg), and HCl (37 wt%, 0.3 mL) into DI water (6 mL) hosted in a glass vial.[3] For the formation of hollow Ru nanoshells, the as-prepared Pd octahedron/Ru array nanostructure sample (1 mL) was added into the etching solution. The mixture was then placed in an oven pre-set to 90 °C and incubated for 3 h. The hollow Ru nanoshells were collected by centrifugation and finally redispersed in DI water.

Preparation of Ru NCs. The preparation method of Ru NCs was similar to that of the Pd octahedron/Ru array nanostructures except that Pd nanooctahedrons were replaced with benzyl alcohol.

Photocatalytic N_2 reduction. The photocatalytic N_2 reduction was conducted in a customized reactor (diameter = 3 cm) with three ends. Two side ends were inlet and outlet for gas flow, while the middle end was equipped with a quartz window on the top for light illumination. Typically, the photocatalyst (0.3 mg) was dispersed into DI water (8 mL). CH_3OH (2 mL) was added as the hole scavenger. High-purity N_2 was bubbled in the mixture solution at a speed of 50 mL·min^{-1} at a pressure of 1 atm for 10 min before each photocatalytic reaction. A continuous Xe lamp (CEL-HXF 300 W) equipped with an AM 1.5 G filter and a 420 nm cutoff filter was employed as the light source. The optical power density was 400 mW cm^{-2}. A circulation cooling system was used to keep the reaction solution temperature at 25 °C. The N_2 photofixation reaction was performed under visible and NIR light irradiation (λ > 420 nm) for 2 h. N_2 was bubbled in the reaction solution at a speed of 50 mL min^{-1} for the entire photocatalytic process. For each 30 min, an aliquot of the reaction solution (0.6 mL) was taken out, and the catalyst was removed by centrifugation. The produced NH_3 in the supernatant was determined using the indophenol-blue method.[4] Each photocatalytic experiment was repeated three times. The action spectrum was acquired by performing the photocatalytic N_2 fixation under the irradiation of different monochromatic light by using an additional bandpass

filter (450, 475, 500, 520, 550, 600 nm) in the typical photocatalytic process. The optical power density was set at 10 mW cm^{-2} for the action spectrum measurements. All the full widths at half-maximum of the bandpass filters are all 20 nm.

Isotope labelling experiments. The isotope experiments were conducted in a customized gastight glass reactor (Fig. S20). To prevent $^{14}N_2$ from the entrance into the reaction system, two gas-washing bottles were connected to the glass reactor. The first gas-washing bottle can filter the possible NH_3 contaminants in $^{15}N_2$ gas, and the second gas-washing bottle can protect reaction system from the entrance of $^{14}N_2$. Prior to the N_2 fixation, the reaction system was purged with Ar gas (99.999%) at a speed of 20 mL min^{-1} for at least 30 min to remove the dissolved air. Then, $^{15}N_2$ is bubbled into the reaction reactor at a speed of 20 mL min^{-1} for another 30 min. The reactor was sealed at 1 atm $^{15}N_2$ gas by closing the inlet and outlet. The N_2 photofixation experiments were conducted for 2 h. The reaction solution was centrifuged once to recover the catalysts. The supernatant (0.5 mL) was then mixed with HCl (1 M, 50 μL) and DMSO-d6 (25 μL). The resultant solution was added in an NMR tube for NMR measurement. The ammonia concentrations were determined by using a Bruker Avance Ⅲ HD 600 NMR spectrometer.

FDTD Simulation. The scattering, absorption and extinction spectra of Pd nanooctahedrons were simulated using FDTD method. The dielectric function of Pd was represented by fitting the data points of E. Palik. Regular octahedrons with different edge lengths were modelled. The refractive index of the surrounding water was set to be 1.33. An electromagnetic pulse was launched to simulate a propagating plane wave interacting with the Pd nanooctahedrons. The scattering and absorption signals were then collected by energy monitors and normalized by the incident light power. The extinction spectra were calculated as the sum of scattering and absorption.

Characterization. TEM imaging was conducted on an HT7700 electron microscope at 100 kV. HRTEM, HAADF-STEM imaging and EDX mapping were carried out on an FEI Themis Z microscopy. The extinction spectra were recorded using a Hitachi U-3900 ultraviolet/visible/NIR spectrophotometer. SEM images were obtained with an FEI field-emission scanning electron microscope (ZEISS Sigma 300) operated at an accelerating voltage of 10 kV. XRD patterns were carried out on a Smart Lab Se diffractometer equipped with Cu Kα radiation. XPS spectra were obtained on a Thermo Scientific ESCALAB 250Xi spectrometer equipped with an Al Kα X-ray source ($h\nu$ = 1486.6 eV). Inductively coupled plasma optical emission spectroscopy (ICP-OES) was measured on a PerkinElmer Optima 7300 DV system. N_2-TPD was carried out on a Micromeritics AutoChem II 2920 system. Steady-state SPV

measurements were conducted on CEL-SPS1000 system. The ion chromatography spectra were measured using a Thermo Scientific ICS-5000+ system. ^{1}H NMR spectra were measured on a Bruker Avance III HD 600 NMR spectrometer. Low-temperature Fourier transform infrared (LT-FTIR) spectra were conducted on Bruker VERTEX 80V at 130 K.

Supplementary Figures

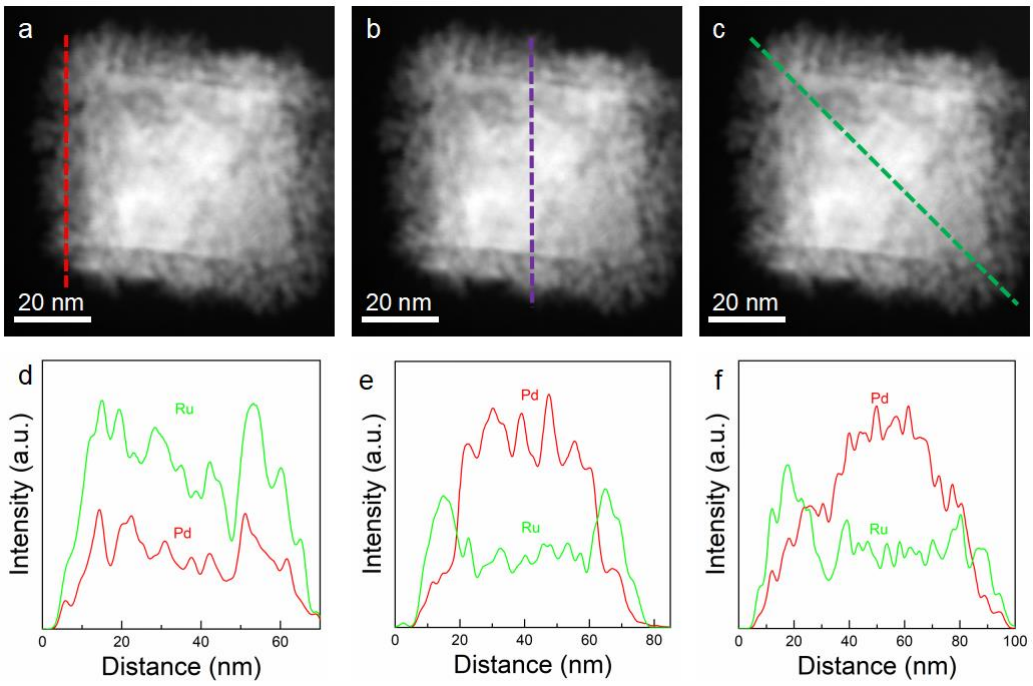

Fig. S1 Elemental profiles of a single Pd octahedron/Ru array nanostructure. (a–c) HAADF-STEM images. (d–e) Elemental profiles of Pd and Ru acquired along the dashed red (a), purple (b) and green (c) lines indicated in (a–c).

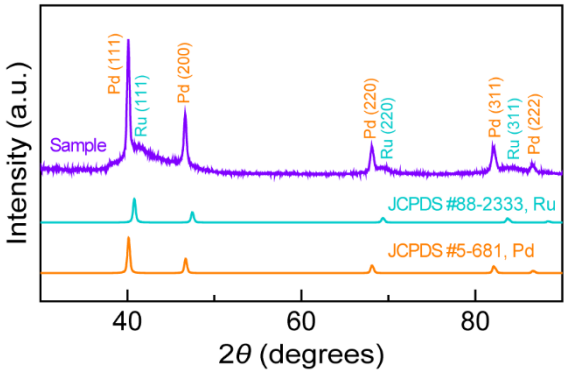

Fig. S2 XRD patterns of a representative Pd octahedron/Ru array nanostructure sample. The orange and cyan curves are the standard powder diffraction patterns of the face-centered-cubic structure of Pd (space group, F*m*-3*m*; lattice constant, 0.38898 nm) and the face-centered-cubic structure of Ru (space group, F*m*-3*m*; lattice constant, 0.383 nm), respectively.

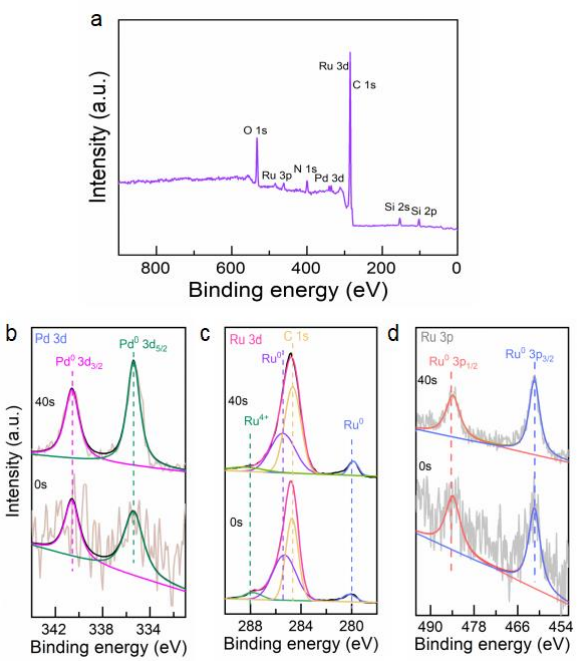

Fig. S3 XPS spectra of a representative Pd octahedron/Ru array nanostructure sample. (a) XPS survey spectrum. (b–d) High-resolution Pd 3d (b), Ru 3d (c), and Ru 3p (d) XPS spectra. The bottom and top spectra are acquired by *in situ* Ar^+ ion sputtering for 0 s and 40 s, respectively.

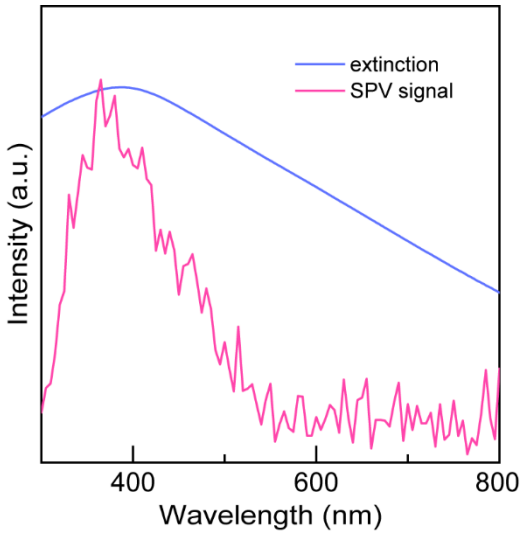

Fig. S4 Extinction (blue) and SPV (red) spectra of Pd nanooctahedrons.

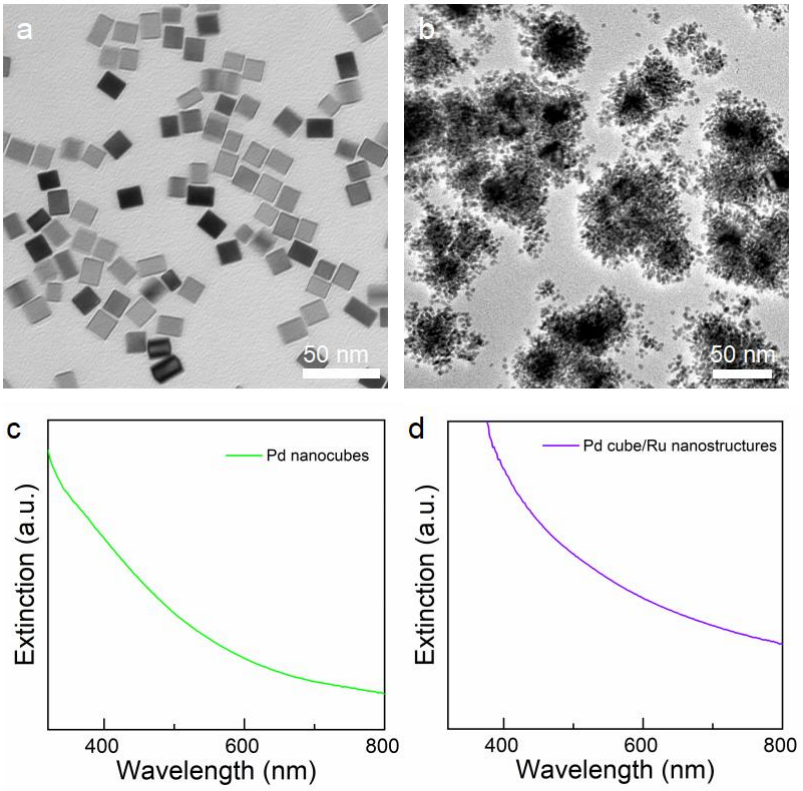

Fig. S5 (a and b) TEM images of Pd nanocube (a) and Pd cube/Ru nanostructure (b) samples. (c and d) Extinction spectra of Pd nanocube (c) and Pd cube/Ru nanostructure (d) samples.

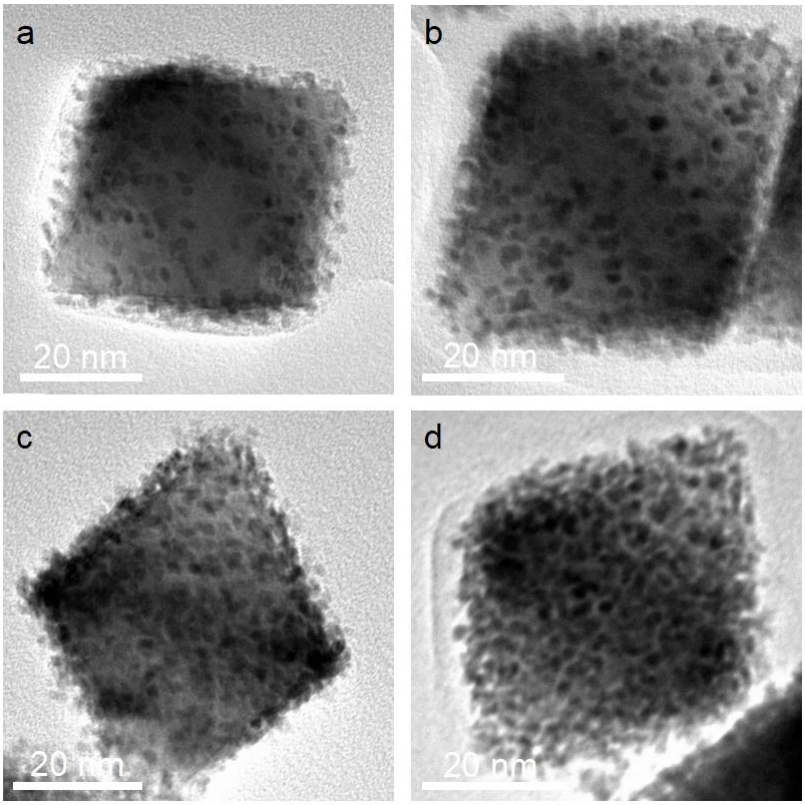

Fig. S6 TEM images of an individual Pd octahedron/Ru array nanostructure obtained by using $Ru(acac)_3$ (2 mL)

with different concentrations as the precursors. (a) 0.25 mg mL^{-1}. (b) 0.5 mg/mL^{-1}. (c) 0.75 mg mL^{-1}. (d) 1 mg mL^{-1}. The gap distances of Ru nanoarrays are 2.5 ± 0.6 nm (a), 1.9 ± 0.3 nm (b), 1.3 ± 0.3 nm (c), and 0.9 ± 0.2 nm (d), respectively.

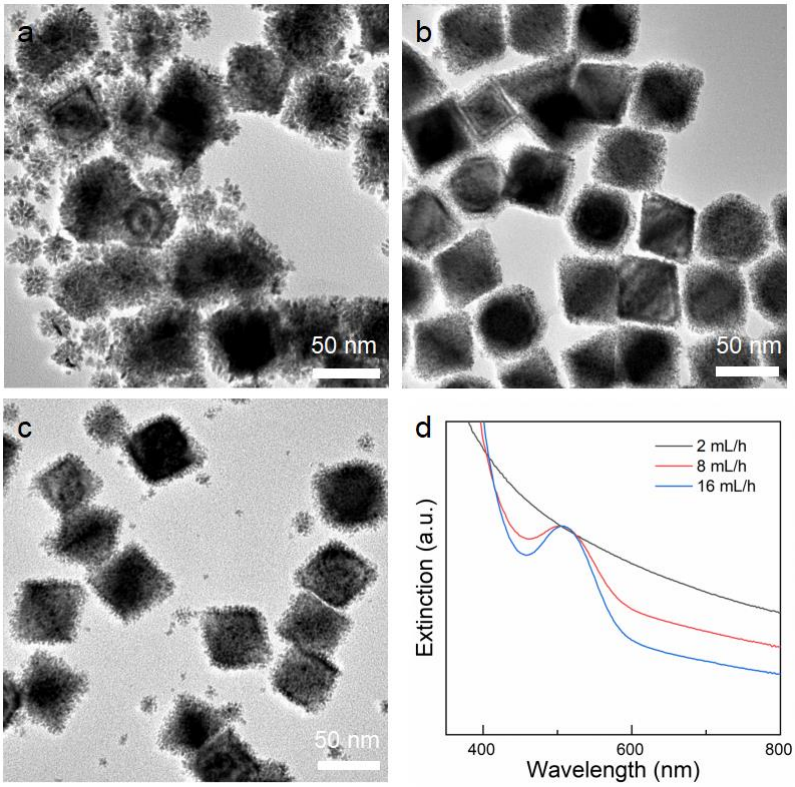

Fig. S7 Effect of the injection rate on the growth behavior. (a–c) TEM images of the Pd octahedron/Ru array nanostructures obtained at a precursor injection rate of 2 mL h^{-1} (a), 8 mL h^{-1} (b), and 16 mL h^{-1} (c), respectively. (d) Extinction spectra of the Pd octahedron/Ru array nanostructures obtained by using varying injection rates.

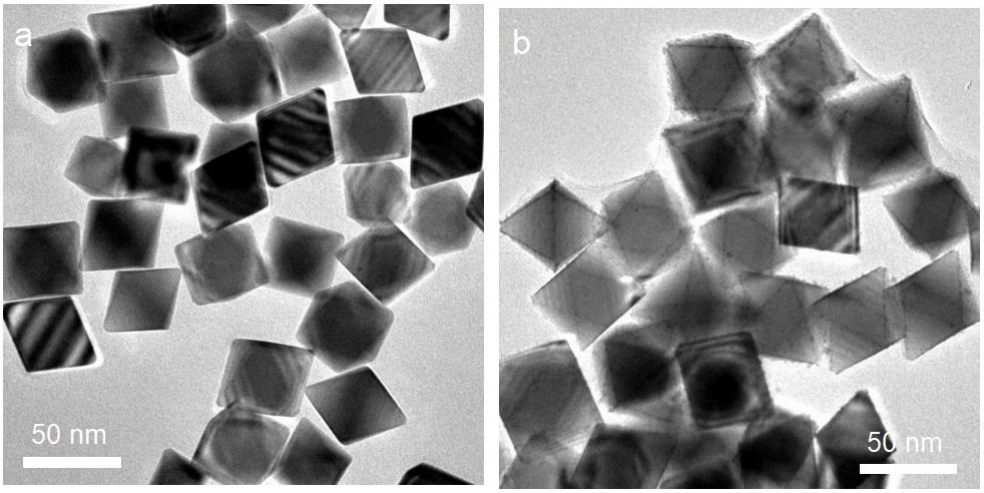

Fig. S8 Effect of the temperature on the growth behavior. (a and b) Representative TEM images of the Pd octahedron/Ru array nanostructures grown at a reaction temperature of 100 °C (a) and 140 °C (b).

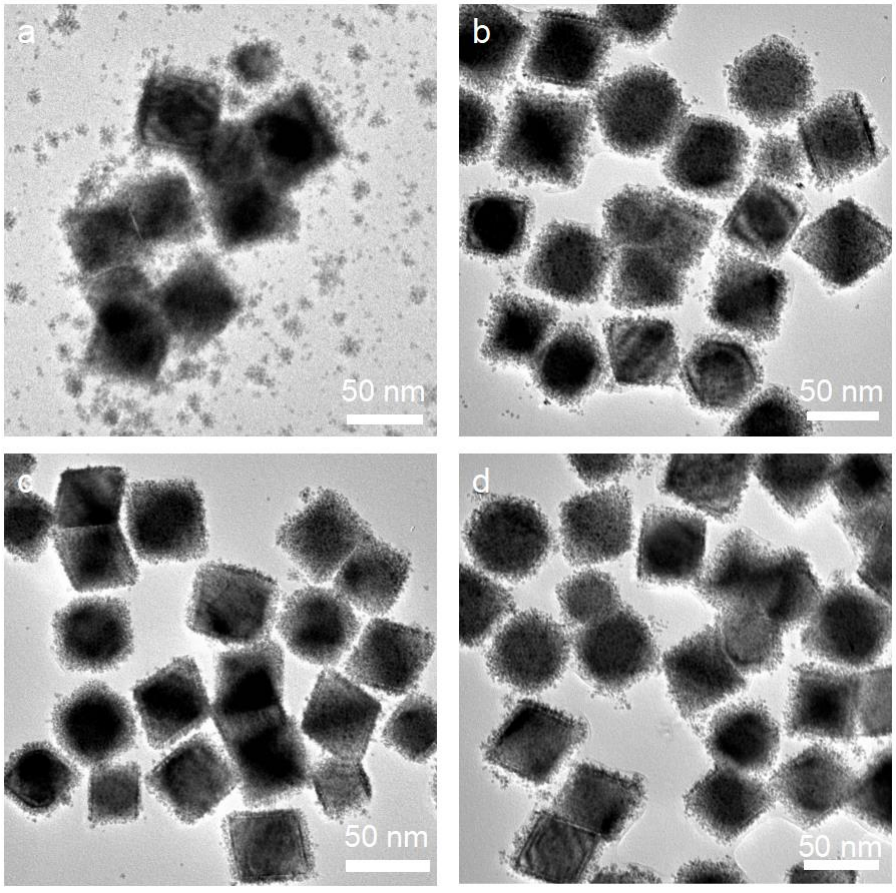

Fig. S9 Effect of the PVP molecular weight on the growth behavior of Ru. (a−d) Representative TEM images of the Pd octahedron/Ru array nanostructures grown with the PVPs with molecular weights of 10000 g mol^{-1} (a), 29000 g mol^{-1} (b), 40000 g mol^{-1} (c), and 130000 g·mol^{-1} (d), respectively.

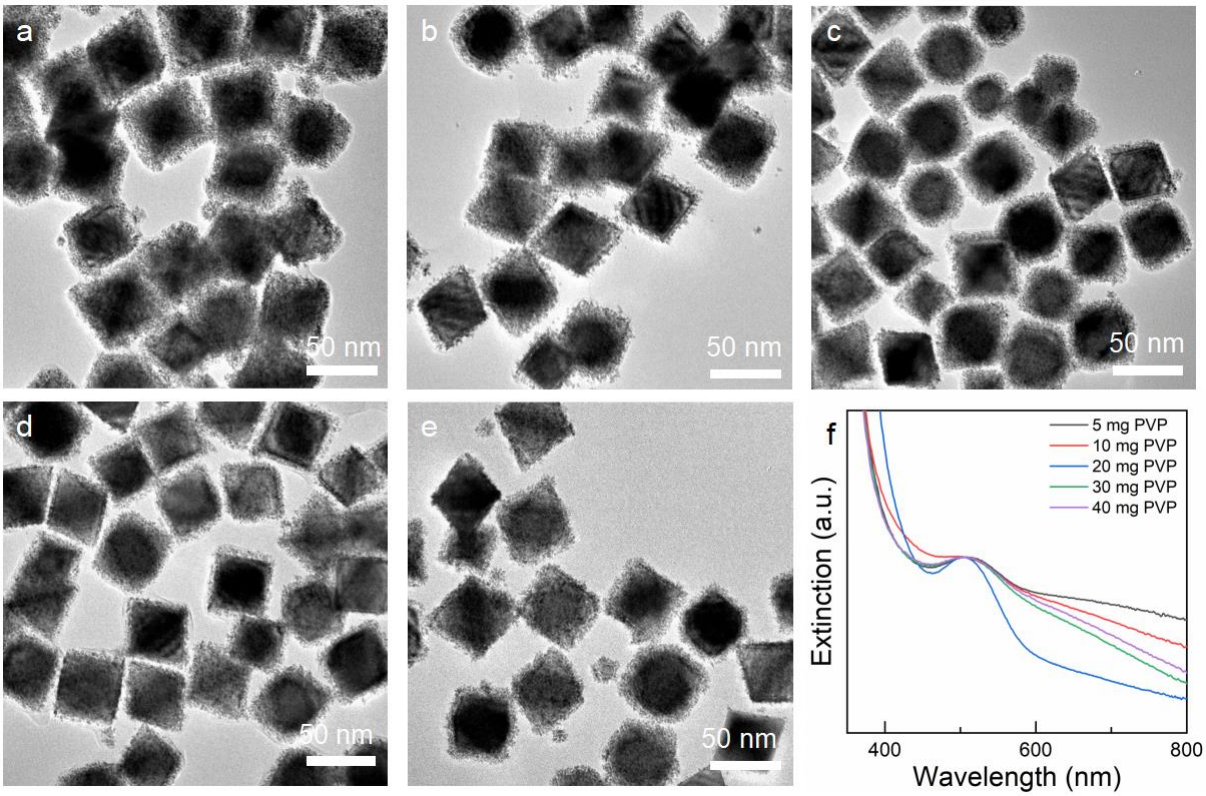

Fig. S10 Effect of the PVP adding amount on the growth behavior. (a–e) TEM images of Pd octahedron/Ru array nanostructures obtained with PVP adding amounts of 5 mg (a), 10 mg (b), 20 mg (c), 30 mg (d), and 40 mg (e), respectively. (f) Extinction spectra of Pd octahedron/Ru array nanostructures obtained using different amounts of PVP.

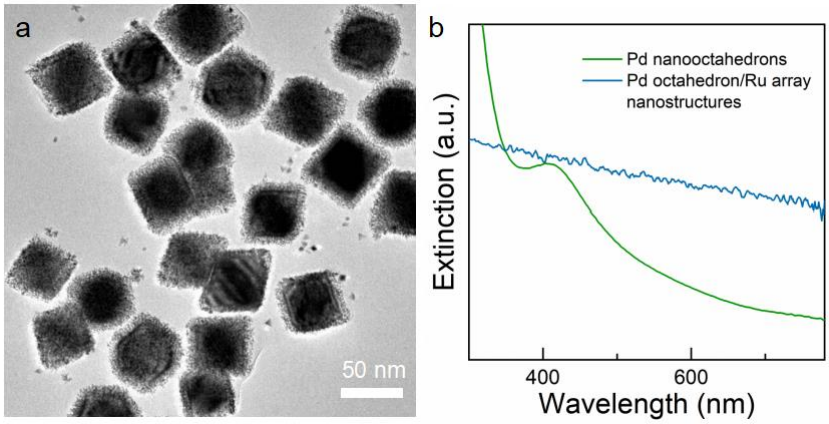

Fig. S11 Effect of the Ru precursor on the growth behavior. (a) TEM image of the Pd octahedron/Ru array nanostructures grown with $RuCl_3$ as the precursor. (b) Extinction spectra of Pd nanooctahedrons (green) and Pd octahedron/Ru array nanostructures (blue) obtained with $RuCl_3$ as the precursor.

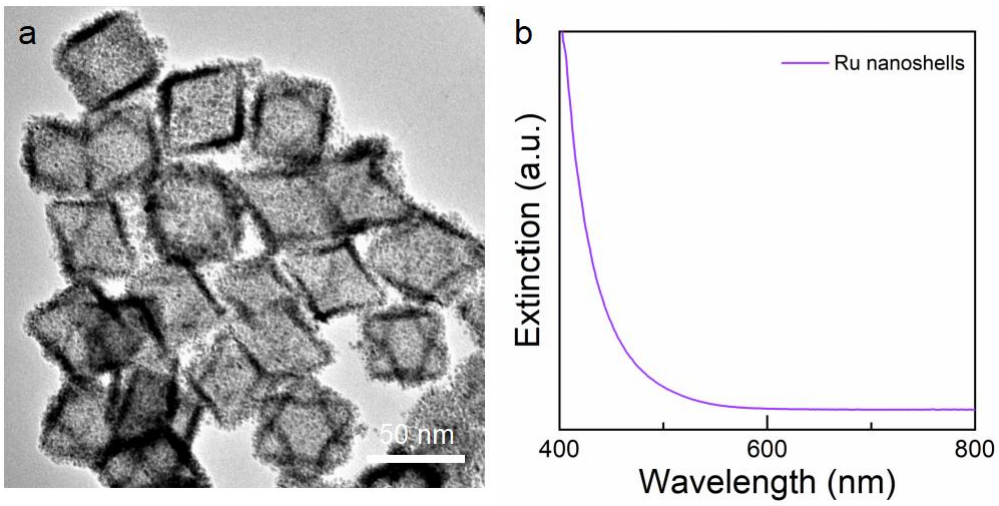

Fig. S12 (a and b) TEM image (a) and extinction spectrum (b) of Ru nanoshells obtained by etching Pd from Pd octahedron/Ru array nanostructures.

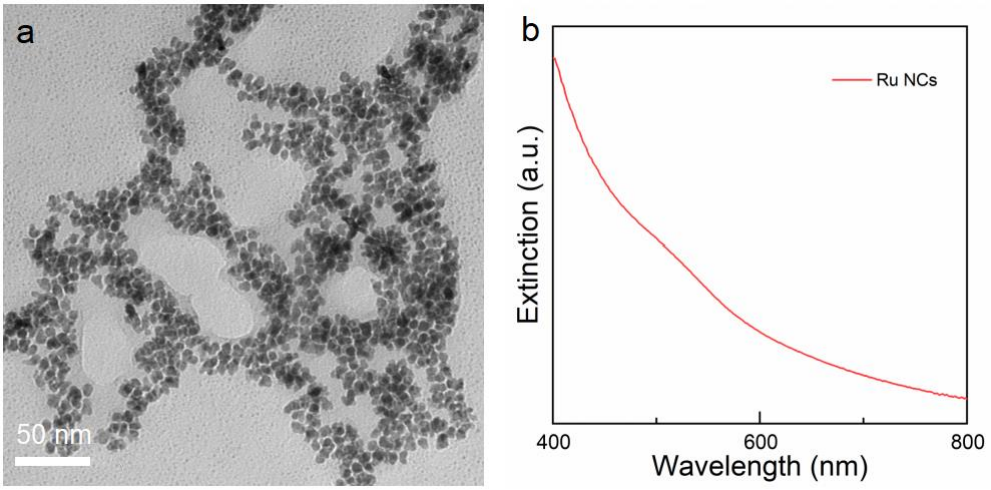

Fig. S13 (a and b) TEM image (a) and extinction spectrum (b) of Ru NCs used for photocatalytic N_2 fixation.

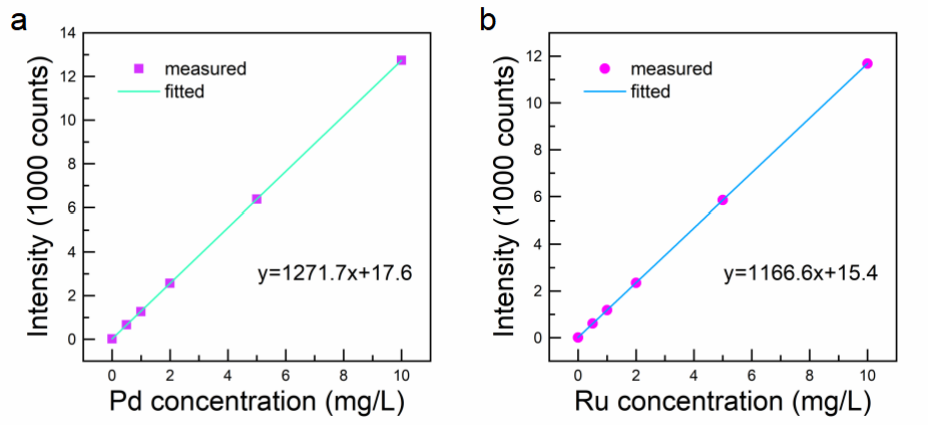

Fig. S14 Linear calibration relationships between the emission intensity and the atomic mass concentration for Pd and Ru in the ICP-OES measurements. (a) For Pd, the coefficient of determination for the linear fitting is R^2 = 0.99999. (b) For Ru, the coefficient of determination for the linear fitting is R^2 = 1.

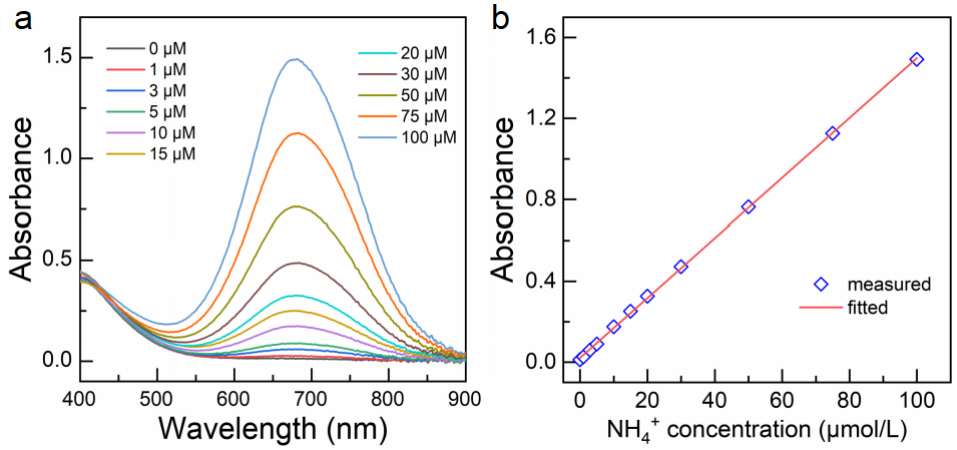

Fig. S15 (a) Absorption spectra of the standard NH_4^+ solutions with different concentrations. (b) Linear relationship between the absorbance values and the standard NH_4^+ solution concentrations. The coefficient of determination for the linear fitting is R^2 = 0.99977.

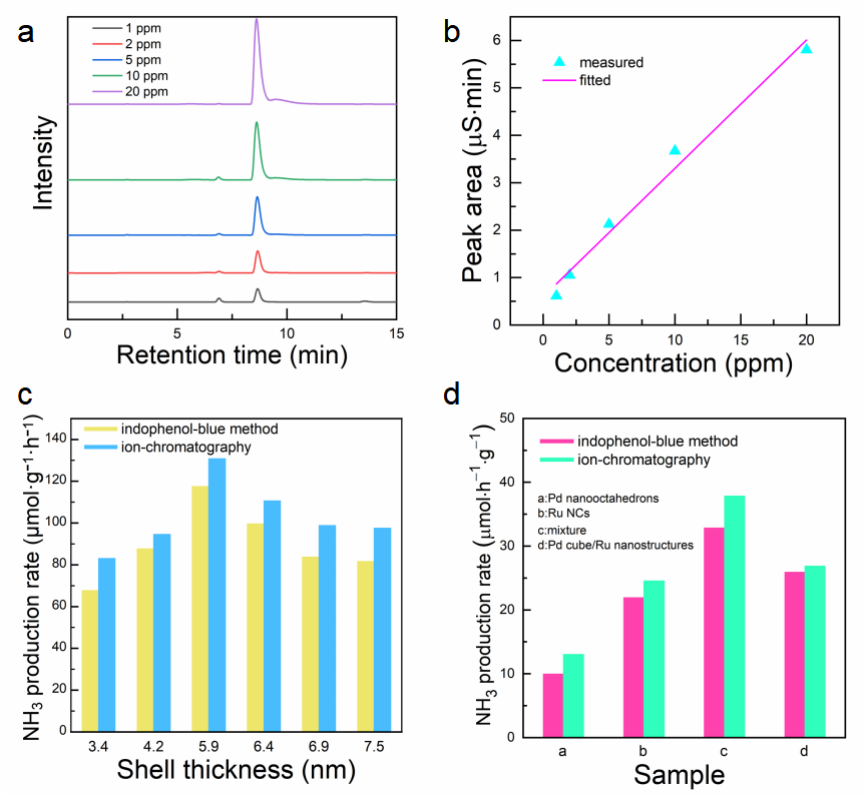

Fig. S16 (a) Ion chromatography spectra of the standard NH_4^+ solutions with different concentrations. (b) Linear relationship between the peak area values and the standard NH_4^+ solution concentrations. (c) The N_2 fixation activities of Pd/Ru samples with different shell thicknesses determined by ion chromatography method and indophenol-blue method. (d) The N_2 fixation activities of different catalysts determined by ion chromatography method and indophenol-blue method.

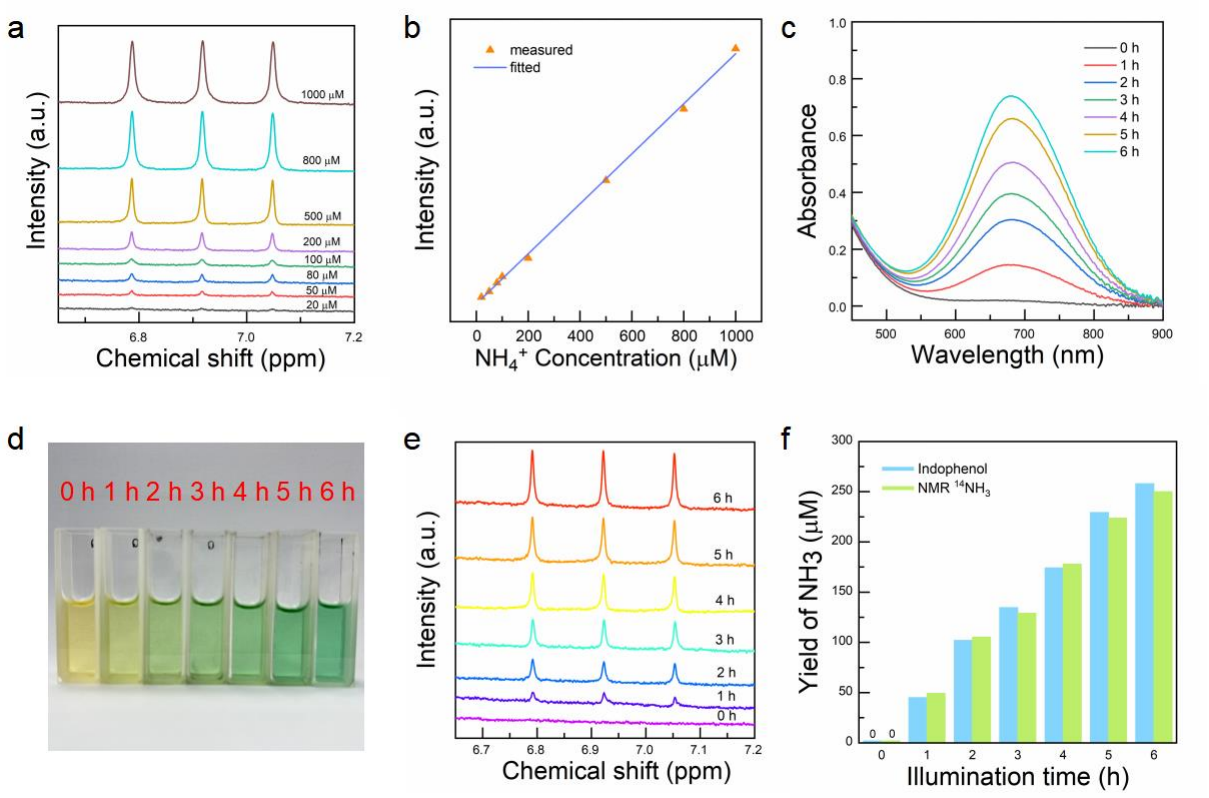

Fig. S17 (a) ^{1}H NMR spectra of the standard NH_4Cl solutions with different concentrations. (b) Linear relationship between the integrated peak areas and the standard NH_4^+ solution concentrations. (c, d) Absorption spectra (c) and photographs (d) of the reaction solutions at different times measured by indophenol blue method. (e) ^{1}H NMR spectra of the reaction solutions at different times. (f) The values of the produced NH_3 at different times determined by indophenol blue method and NMR method.

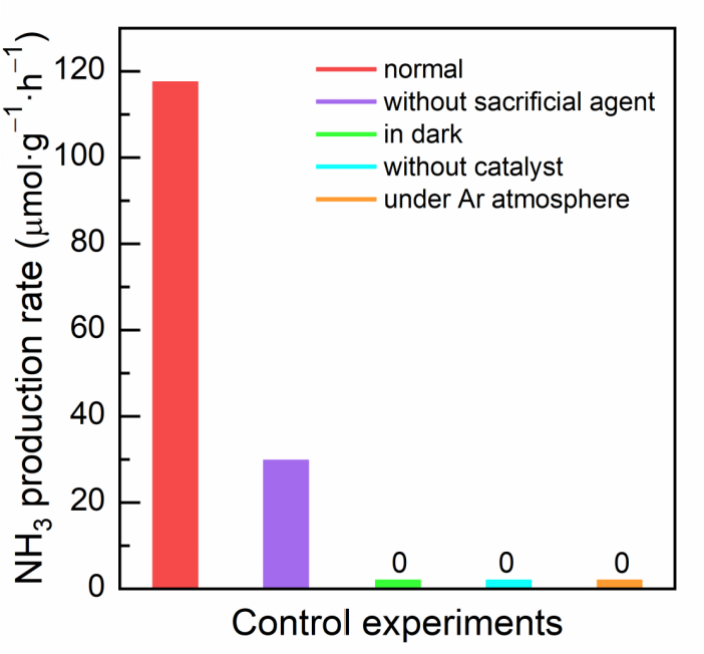

Fig. S18 Control experiments of the N_2 photofixation under different conditions.

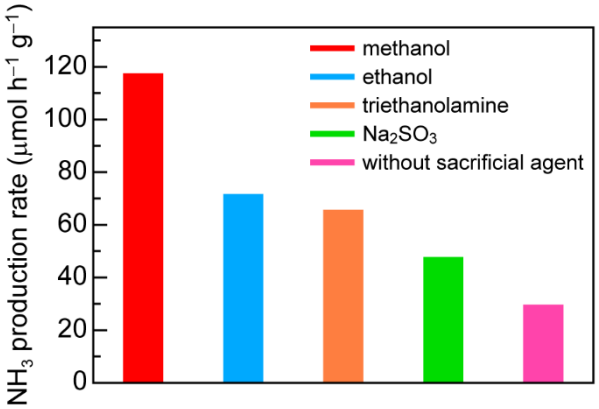

Fig. S19 Effect of the hole sacrificial reagents.

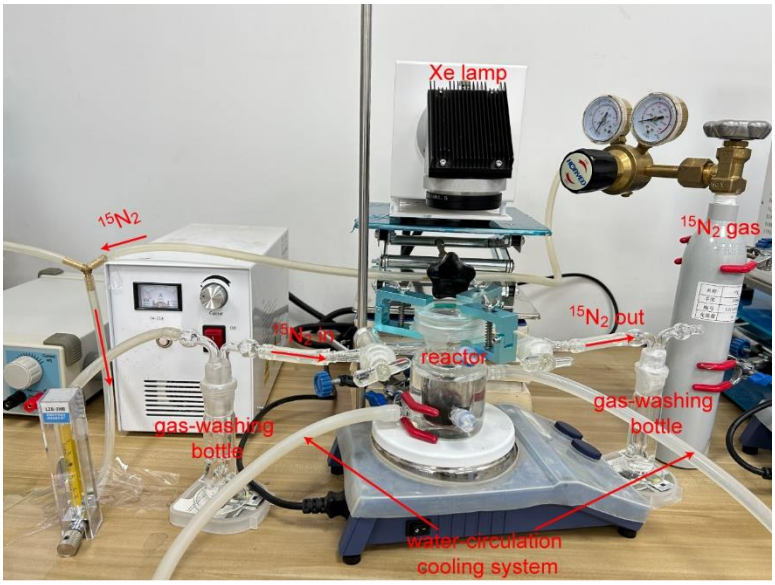

Fig. S20 Photograph of the photocatalytic system for the isotope labelling experiments.

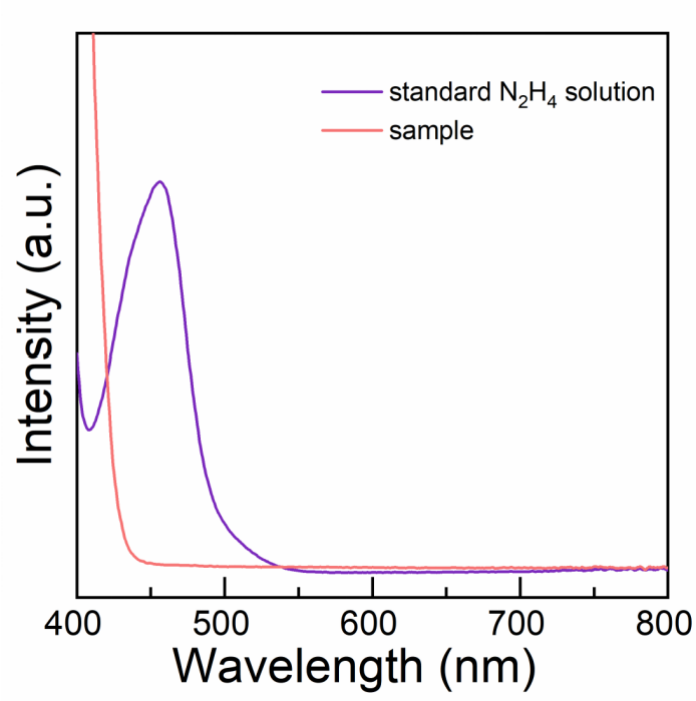

Fig. S21 Detection of the possible N_2H_4 byproduct.

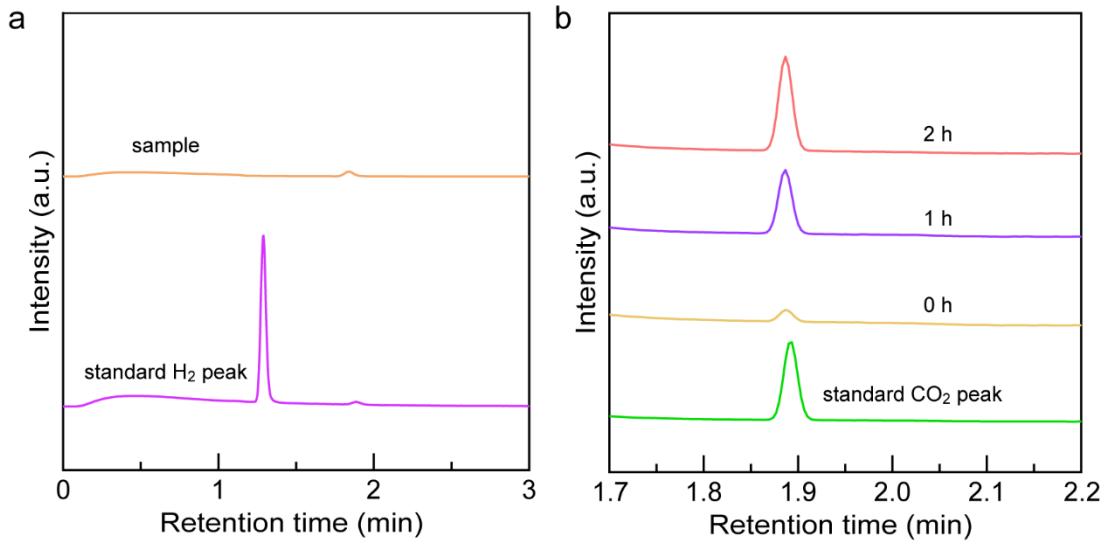

Fig. S22 (a, b) Detection of the possible H_2 (a) or CO_2 (b) evolution in the photocatalytic process.

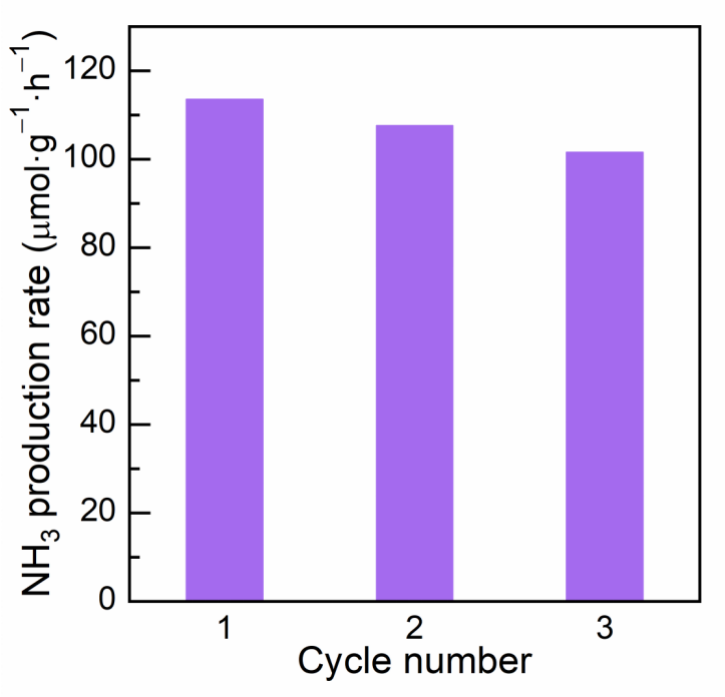

Fig. S23 NH_3 production rates during three successive cycles. The reaction time is 2 h for each cycle.

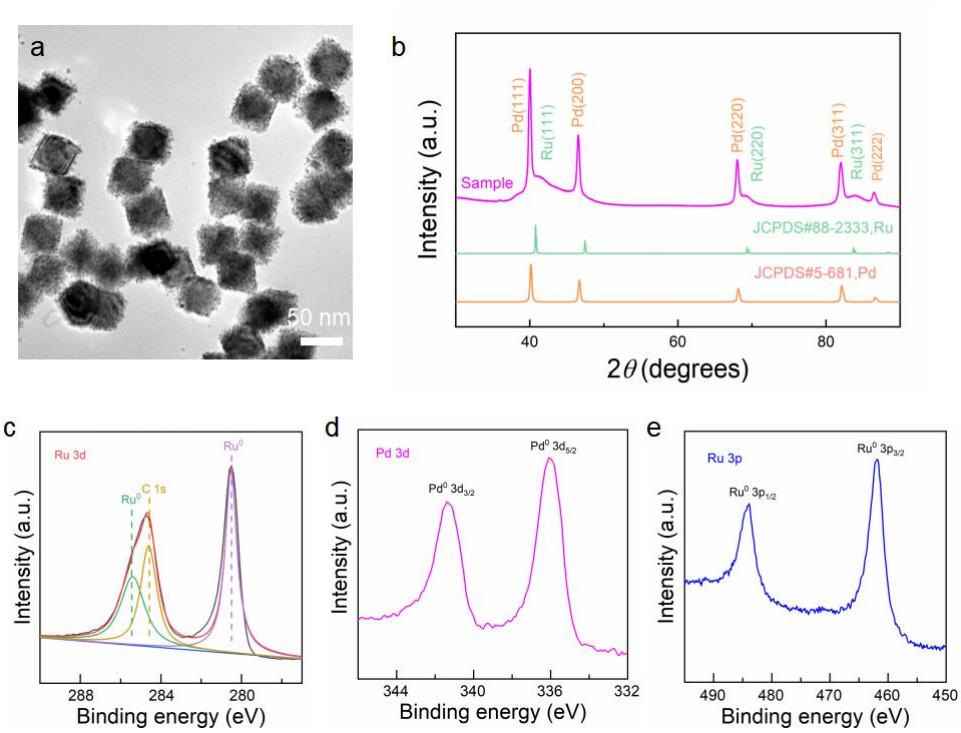

Fig. S24 TEM image (a) and XRD patterns (b) of the Pd octahedron/Ru array nanostructures after the photocatalytic process. (c–e) High-resolution Ru 3d (b), Pd 3d (c), and Ru 3p (d) XPS spectra of the Pd octahedron/Ru array nanostructures after the typical photocatalytic reaction.

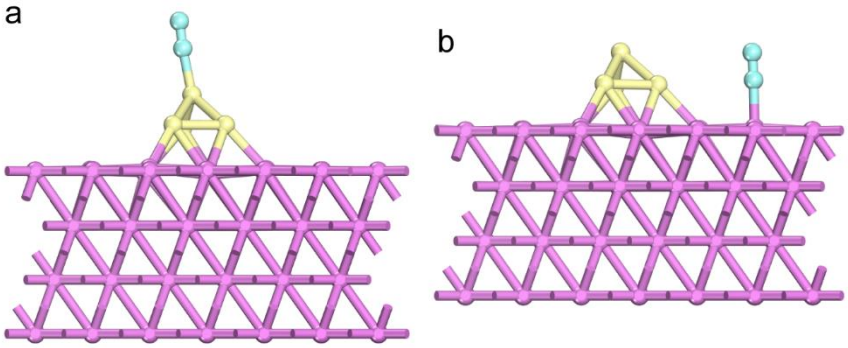

Fig. S25 Adsorption configurations of a N_2 molecule at Ru (a) and Pd (b) sites on the Pd octahedron/Ru array nanostructures.

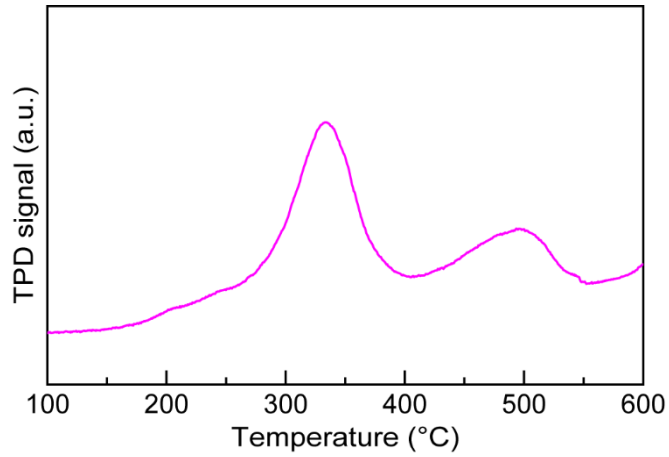

Fig. S26 N_2 TPD profile of the Pd octahedron/Ru array nanostructures.

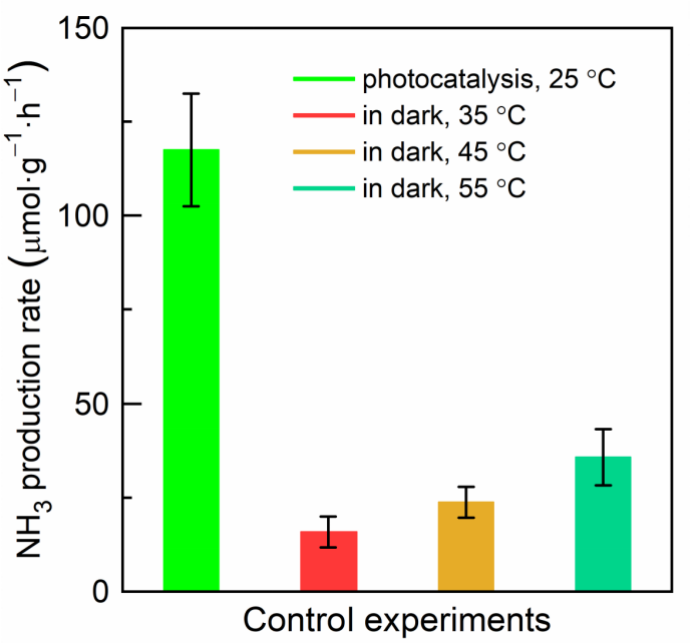

Fig. S27 N_2 photofixation experiments under different temperatures.

Supplementary Table

Table S1. The weighs of the different catalysts used for the N_2 photofixation.

catalyst	mass of Pd (μg)	mass of Ru (μg)	Total mass (μg)	Molar ratio of Pd to Ru
$Pd/Ru_{7.5}$	264.9	54.7	319.6	82:18
$Pd/Ru_{6.9}$	277.3	52.0	329.3	84:16
$Pd/Ru_{6.4}$	279.7	48.0	327.7	85:15
$Pd/Ru_{5.9}$	282.7	44.3	327.0	86:14
$Pd/Ru_{4.2}$	264.0	33.8	297.8	88:12
$Pd/Ru_{3.4}$	290.4	29.7	320.1	90:10
Pd nanooctahedrons	320.2	0	320.2	
Ru NCs	0	280.0	280.0	
mixture of Pd nanooctahedrons and Ru NCs	320.2	28.0	348.2	92:8
Pd cube/Ru nanostructures	265.8	29.9	295.7	89:11

References

1. M. C. Liu, Y. Q. Zheng, L. Zhang, L. J. Guo and Y. N. Xia, *J. Am. Chem. Soc.*, 2013, **135**, 11752−11755.

2. M. S. Jin, H. Zhang, Z. X. Xie and Y. N. Xia, *Energy Environ. Sci.*, 2012, **5**, 6352−6357.

3. H. H. Ye, Q. X. Wang, M. Catalano, N. Lu, J. Vermeylen, M. J. Kim, Y. Z. Liu, Y. G. Sun and X. H. Xia, *Nano Lett.*, 2016, **16**, 2812−2817.

4. J. H. Yang, Y. Z. Guo, R. B. Jiang, F. Qin, H. Zhang, W. Z. Lu, J. F. Wang and J. C. Yu, *J. Am. Chem. Soc.*, 2018, **140**, 8497−8508.